

## Leesite, $\text{K}(\text{H}_2\text{O})_2[(\text{UO}_2)_4\text{O}_2(\text{OH})_5]\cdot 3\text{H}_2\text{O}$ , a new K-bearing schoepite-family mineral from the Jomac mine, San Juan County, Utah, U.S.A.

TRAVIS A. OLDS<sup>1,\*</sup>, JAKUB PLÁŠIL<sup>2</sup>, ANTHONY R. KAMPF<sup>3</sup>, TYLER SPANO<sup>1</sup>, PATRICK HAYNES<sup>4</sup>, SHAWN M. CARLSON<sup>5</sup>, PETER C. BURNS<sup>1,6</sup>, ANTONIO SIMONETTI<sup>1</sup>, AND OWEN P. MILLS<sup>7</sup>

<sup>1</sup>Department of Civil and Environmental Engineering and Earth Sciences, University of Notre Dame, Notre Dame, Indiana 46556, U.S.A.

<sup>2</sup>Institute of Physics ASCR, v.v.i., Na Slovance 1999/2, 18221 Prague 8, Czech Republic

<sup>3</sup>Mineral Sciences Department, Natural History Museum of Los Angeles County, 900 Exposition Boulevard, Los Angeles, California 90007, U.S.A.

<sup>4</sup>901 Sean Street, Socorro, New Mexico 87801, U.S.A.

<sup>5</sup>245 Jule Lake Road, Crystal Falls, Michigan 49920, U.S.A.

<sup>6</sup>Department of Chemistry and Biochemistry, University of Notre Dame, Notre Dame, Indiana 46556, U.S.A.

<sup>7</sup>Applied Chemical and Morphological Analysis Laboratory, Michigan Technological University, Houghton, Michigan 49931, U.S.A.

### ABSTRACT

Leesite (IMA2016-064),  $\text{K}(\text{H}_2\text{O})_2[(\text{UO}_2)_4\text{O}_2(\text{OH})_5]\cdot 3\text{H}_2\text{O}$ , is a new uranyl-oxide hydroxyl-hydrate found underground in the Jomac mine, Brown's Rim, White Canyon mining district, San Juan County, Utah. Laser ablation-inductively coupled plasma-mass spectrometry (LA-ICP-MS) analyses provided the empirical formula  $\text{K}_{0.67}\text{Na}_{0.004}\text{Ca}_{0.012}\text{U}_4\text{O}_{20}\text{H}_{15.31}$ , based on 4 U and 20 O apfu. Sheets in the crystal structure of leesite adopt the fourmarierite anion topology, and so belong to the schoepite family of related structures that differ in the interlayer composition and arrangement, and charge of the sheet. Leesite may form as one of the principal components of "gummite" mixtures formed during the alteration of uraninite, and the unit cell of leesite resembles the previously described, but poorly understood mineral, paraschoepite. Uptake of dangerous radionuclides (<sup>90</sup>Sr, <sup>135</sup>Cs, <sup>137</sup>Cs, <sup>237</sup>Np, <sup>238</sup>Pu) into the structure of leesite and other members of the family has important implications for the safe disposal of nuclear waste.

**Keywords:** Leesite, sheet anion topology, schoepite, uranium, uraninite, crystal structure

### INTRODUCTION

Uranium dioxide nuclear fuel and uraninite,  $\text{UO}_{2+x}$ , readily alter in the presence of water and oxygen leading to the formation of uranyl-oxide hydroxyl-hydrate minerals (UOH) (Finch and Ewing 1992; Wronkiewicz et al. 1992). UOH minerals are among the first phases to form during the oxidation-hydration weathering of  $\text{UO}_2$  (Finch et al. 1996a; Plášil 2014), and studies detailing their structure, solubility, and stability are numerous due to their importance for nuclear waste disposal and the environmental chemistry of uranium in general (Amonette et al. 1994; Finch and Murakami 1999; Klingensmith et al. 2007; Kubatko et al. 2006). Schoepite,  $[(\text{UO}_2)_8\text{O}_2(\text{OH})_{12}]\cdot 12\text{H}_2\text{O}$ , the most hydrous UOH, was described by Walker (1923) nearly 95 years ago, yet the crystal-chemical details of phases produced during its dehydration are still uncertain. Different minerals form depending on the rate of dehydration, and the presence of cations can impart variable  $(\text{OH}^-)$  content in the sheets that build UOH minerals (Table 1). The structures of several of these minerals are built from the same sheet topology found in schoepite (Finch et al. 1996b), and the so-named schoepite family includes schoepite, metaschoepite,  $[(\text{UO}_2)_4\text{O}(\text{OH})_6]\cdot 5\text{H}_2\text{O}$  (Weller et al. 2000), fourmarierite,  $\text{Pb}[(\text{UO}_2)_4\text{O}_3(\text{OH})_4]\cdot 4\text{H}_2\text{O}$  (Li and Burns 2000), paraschoepite,  $\text{UO}_3\cdot 1.9\text{H}_2\text{O}$  (Schoep and Stradiot 1947),

paulscherrite,  $\text{UO}_2(\text{OH})_2$  (previously "dehydrated-schoepite") (Brugger et al. 2011), and heisenbergite,  $\text{UO}_2(\text{OH})_2\cdot \text{H}_2\text{O}$  (Walenta and Theye 2012). Describing the crystallography of these minerals has been challenging due to the lack of suitably pure material, in sufficiently large crystals. Leesite is a new member of the schoepite family containing monovalent cations in the interlayer and marks the 22nd addition to the family of uranyl-oxide hydroxyl-hydrate minerals. Plášil et al. (2016) give an updated listing of the members of this family. Herein, we provide a description of the crystal structure of leesite and observations regarding substitutional variability between other members of the family, including Na-rich metaschoepite and K-rich fourmarierite from Jáchymov, Czech Republic.

The name leesite honors American mineral dealer and collector Bryan K. Lees (born 1957). Lees received his B.S. in Geological Engineering from the Colorado School of Mines in 1985. In the same year, he founded Collector's Edge Minerals, through which he has developed innovative specimen extraction techniques and created what is probably the world's most advanced collector-specimen preparation laboratory. In the 1990s, Lees spearheaded the mining of rhodochrosite at Colorado's Sweet Home mine. The rhodochrosite samples produced by this venture are widely considered to be some of the most valuable non-gem mineral specimens ever found, and many were personally collected with his advanced extraction techniques. Lees has conducted 40 specimen-mining projects on five continents and

\* E-mail: tolds@nd.edu

**TABLE 1.** Unit-cell parameters for analogous uranyl-oxide hydroxide hydrate phases

Phase	Occurrence	<i>a</i> (Å)	<i>b</i> (Å)	<i>c</i> (Å)	<i>V</i> (Å <sup>3</sup> )	Space Group	$\Sigma_M$ s.o.f.
<b>Neutral sheets</b>							
Schoepite <sup>a</sup>	Shaba, DRC	14.337(3)	16.813(5)	14.731	3426(7)	<i>P2<sub>1</sub>ca</i>	0
Metaschoepite <sup>b</sup>	Shaba, DRC	14.680(2)	14.029(2)	16.720(1)	3443	<i>Pbcn</i>	0
Metaschoepite <sup>c</sup>	synthetic	14.6861(4)	13.9799(3)	16.7063(5)	3439	<i>Pbcn</i>	0
Paraschoepite <sup>d</sup>	Shinkolobwe, DRC	14.12	16.83	15.22	3617	<i>Pbca</i>	0
Heisenbergite <sup>e</sup>	Menzenschwand, DE	13.10(1)	13.76(1)	14.50(1)	2613.7(2)	<i>P2<sub>1</sub>2<sub>1</sub>2<sub>1</sub>; Pna2<sub>1</sub></i>	0
Paulscherrerite <sup>f</sup>	Radium Ridge, AU	4.288(2)	10.270(6)	6.885(5)	303.2(2)	<i>P2<sub>1</sub>; P2<sub>1</sub>/m</i>	0
$\alpha$ -UO <sub>2</sub> (OH) <sub>2</sub> <sup>g</sup>	synthetic	4.242(1)	10.302(1)	6.868(1)	300.1(1)	<i>Cmca</i> or <i>C2cb</i>	0
<b>Charged sheets</b>							
Leesite <sup>h</sup>	Utah, U.S.A.	14.866(7)	14.126(7)	16.772(8)	3522(3)	<i>Pbca</i>	0.71
Na-rich metaschoepite <sup>i</sup>	synthetic	14.7050(6)	14.0565(5)	16.7051(6)	3453	<i>Pbcn</i>	0.545
Na-rich metaschoepite <sup>j</sup>	Jáchymov, CZ	14.64(2)	14.03(1)	16.69(2)	3426(7)	<i>Pbcn</i>	0.91
K-rich fourmarierite <sup>k</sup>	Jáchymov, CZ	14.025(2)	16.469(4)	14.623(2)	3378(2)	<i>Bb2<sub>1</sub>m</i>	0.96
K-rich fourmarierite <sup>l</sup>	Jáchymov, CZ	13.442(5)	16.611(6)	14.447(2)	3226(1)	<i>Bb2<sub>1</sub>m</i>	1.03
Fourmarierite <sup>k</sup>	Shinkolobwe, DRC	14.010(1)	16.401(1)	14.317(1)	3290	<i>Bb2<sub>1</sub>m</i>	1.022
Fourmarierite <sup>k</sup>	Shinkolobwe, DRC	14.018(1)	16.468(1)	14.368(1)	3317	<i>Bb2<sub>1</sub>m</i>	0.863
Fourmarierite <sup>k</sup>	synthetic	13.938(2)	16.638(3)	14.672(2)	3402	<i>Bb2<sub>1</sub>m</i>	0.497
Kroupaite <sup>l</sup>	Jáchymov, CZ	14.8201(8)	14.0958(8)	16.765(1)	3502.3(3)	<i>Pbca</i>	0.69

<sup>a</sup> Finch et al. (1996b), <sup>b</sup> Klingensmith et al. (2007), <sup>c</sup> Weller et al. (2000), <sup>d</sup> Schoep and Stradiot (1947), <sup>e</sup> Walenta and Theye (2012), <sup>f</sup> Brugger et al. (2011), <sup>g</sup> Taylor and Hurst (1971), <sup>h</sup> This work, <sup>i</sup> Klingensmith et al. (2007), <sup>j</sup> Sejkora et al. (2013), <sup>k</sup> Li and Burns (2000), <sup>l</sup> Plášil et al. (2017).

his samples are displayed in the collections of museums and individuals around the world. For his accomplishments, he has received the Friends of Mineralogy Author of the Year Award (1998), Carnegie Mineralogical Award (1998), the Colorado School of Mines Medal (2003), and the American Mineral Heritage Award (2014).

The Commission on New Minerals, Nomenclature and Classification of the International Mineralogical Association approved the new mineral and name (IMA2016-064). The description is based upon two co-type specimens from the Jomac mine, deposited in the Natural History Museum of Los Angeles County, California, U.S.A., with catalog numbers 66285 and 66286.

## OCCURRENCE

Leesite is found underground in the Jomac mine, Brown's Rim, White Canyon mining district, San Juan County, Utah (37°51'43"N 110°19'10"W), about 5.5 km SE of Hite Crossing. Material containing the new mineral was collected in 1989 by one of the authors (P.H.). The Jomac mine consisted of three adits that are now closed and reclaimed. Collecting has been prohibited since 1992 when the area was incorporated into the Glen Canyon National Recreation Area. Leesite was found in a seam of gypsum, closely associated with compregnacite, K<sub>2</sub>[(UO<sub>2</sub>)<sub>6</sub>O<sub>4</sub>(OH)<sub>6</sub>]·7H<sub>2</sub>O, and a later generation of blatonite UO<sub>2</sub>CO<sub>3</sub>·H<sub>2</sub>O (Vochten and Deliens 1998) and owsaldpeetersite (UO<sub>2</sub>)<sub>2</sub>CO<sub>3</sub>(OH)<sub>2</sub>·4H<sub>2</sub>O (Vochten et al. 2001), two minerals for which the Jomac mine is the type locality. Other accessory minerals include alunite, chalcoalumite, probable mbobomkulite or nickelalumite, sklodowskite, and boltwoodite. The deposit of uranium exploited by the Jomac mine lies in the Shinarump conglomerate member of the Triassic Chinle Formation. An account of the geology and history of the mine is given by Trites and Hadd (1958). Haynes (2000) summarizes this paper, and includes the descriptions of minerals identified up to that time, including two then unknown U minerals (designated "Unknown number 1" and "Unknown number 2"). Unknown number 2 has since been described as owsaldpeetersite and Unknown number 1 is described herein as the new mineral leesite.

## PHYSICAL AND OPTICAL PROPERTIES

Leesite forms as aggregates of orange-yellow tablets up to 1 mm in diameter (Fig. 1). Tablets are flattened and stacked on {100}, the only well-developed crystal form (Fig. 2). Leesite also occurs as powdery masses in the interstices of gypsum crystals. Crystals are brittle with perfect cleavage on {100} and uneven fracture. No twinning was observed. Crystals are translucent with a vitreous luster, give a light yellow streak, and are non-fluorescent under LW and SW UV. The Mohs hardness is approximately 2, estimated by the behavior of crystals when broken. The density was not measured due to the limited availability of material. The calculated density is 3.256 g/cm<sup>3</sup> based on the empirical formula. Leesite is readily soluble in dilute HCl and HNO<sub>3</sub>, with no effervescence.

Leesite is optically biaxial (−), with  $\alpha = 1.745(2)$ ,  $\beta = 1.761(2)$ ,  $\gamma = 1.765(2)$  (measured in white light). The  $2V$  is 50(2)°, measured directly by conoscopic observation on a spindle stage; the calculated  $2V$  is 52.7°. Dispersion is strong,  $r > v$ . The mineral is pleochroic with  $X$  nearly colorless,  $Y$  and  $Z$  orange yellow;  $X < Y \approx Z$ . The optical orientation is  $X = \mathbf{a}$ ,  $Y = \mathbf{c}$ ,  $Z = \mathbf{b}$ . The Gladstone-Dale compatibility,  $1 - (K_p/K_c)$ , is 0.037 (excellent) for the ideal formula, and 0.028 (excellent) for the empirical formula (Mandarino 2007). Raman and Fourier transform infrared spectra of leesite can be accessed online as Supplementary material (Appendix<sup>1</sup> Figs. S1, S2, and S3).

## Chemical composition

Electron microprobe analyses were deemed to be unreliable due to instability and decomposition of crystals under the electron beam. Instead, six chemical analyses were performed using laser ablation-inductively coupled plasma-mass spectrometry (LA-ICP-MS). Six crystal aggregates were embedded in epoxy and polished to provide a flat surface (~50 × 50 μm). The ion signals for U, K, Pb, Na, and Ca were measured using an Element2 sector field high-resolution inductively coupled plasma mass spectrometer (Thermo-Fisher Scientific) in medium mass resolution mode coupled with a UP-213 (New Wave Research) Nd:YAG deep UV (213 nm) laser ablation system. Prior to the laser of samples, the Element2 was

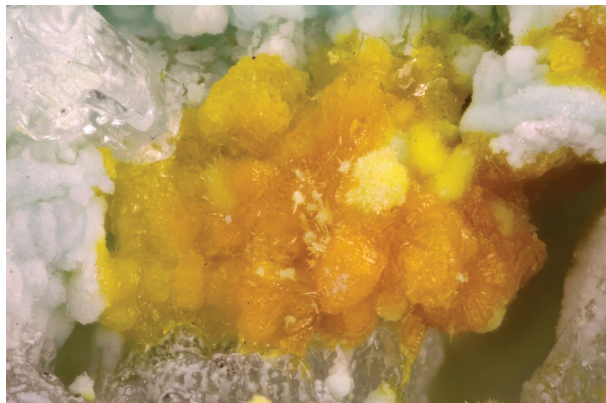


**FIGURE 1.** Orange-yellow aggregates of leesite rim the edges of blocky orange compreignacite, with pale yellow sklodowskite. The whole assemblage sits atop colorless gypsum, with probable white nickellalumite or mbobomkulite. Horizontal field of view is 2 mm. (Color online.)

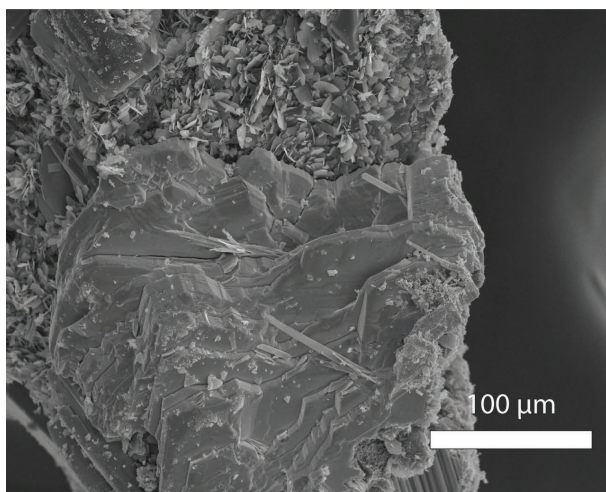


**FIGURE 2.** Secondary electron image of tabular leesite stacked along (100). Photo by Shawn M. Carlson and Owen P. Mills.

tuned using a multi-element solution containing 1 ng/g of each Li, In, and U to obtain maximum ion sensitivity. Laser ablation analyses involved acquiring background ion signals for 60 s with the laser on and shuttered, and this was followed by 60 s of data acquisition. Laser operating conditions involved using an 8  $\mu\text{m}$  spot size, repetition rate of 5 Hz, 100% power out, which corresponded to a fluence of  $\sim 8.4 \text{ J/cm}^2$ . Six areas on six crystals were examined using a raster scan or single spot analyses depending on the size of the crystals. Leesite contains appreciable U, K, Ca, some Na, and negligible Pb, and the data are given in Table 2. No other elements were detected. The ion signals (cps = counts per second) obtained for K, Ca, and Na are reported as a ratio relative to that recorded for U, as absolute abundances could not be determined due to a lack of an appropriate matrix matched external standard. The  $\text{H}_2\text{O}$  content was calculated according to the structure on the basis of 20 O apfu with charge-balance considerations. The empirical formula,  $\text{K}_{0.67}\text{Na}_{0.004}\text{Ca}_{0.012}\text{U}_4\text{O}_{20}\text{H}_{15.31}$ , is calcu-

**TABLE 2.** LA-ICP-MS data (wt%) for leesite, average of six analyses

Element	Mean ratio (U/cation)	Range	SD	Mean apfu	Calculated wt% oxide
Na	0.001	0.0006–0.0014	0.0004	0.004	–
Ca	0.003	0–0.006	0.482	0.012	–
K	0.168	0.1632–0.1748	0.0042	0.670	2.4
U <sup>a</sup>	1.000	–	–	4	87.09 (as $\text{UO}_3$ )
$\text{H}_2\text{O}^b$	–	–	–	–	10.51

Notes: The element ratios above are alternatively expressed in calculated wt% oxide in the last column, based on the mean apfu derived from the count ratios for each element.

<sup>a</sup> Ratios normalized to 4 U apfu.

<sup>b</sup> Calculated according to the structure with charge-balance considerations on the basis of 20 O apfu.

lated on the basis of 4 U and 20 O apfu. The ideal formula is  $\text{K}(\text{H}_2\text{O})_2[(\text{UO}_2)_4\text{O}_2(\text{OH})_5] \cdot 3\text{H}_2\text{O}$ , which requires:  $\text{K}_2\text{O}$  3.55,  $\text{UO}_3$  86.27,  $\text{H}_2\text{O}$  10.18, total 100 wt%.

### Single-crystal X-ray diffraction and refinement

A homogenous plate fragment with sharp optical extinction in cross-polarized light was chosen for single-crystal X-ray diffraction study. Data were collected using  $\text{MoK}\alpha$  X-rays from a microfocus source and an Apex II CCD-based detector mounted to a Bruker Apex II Quazar three-circle diffractometer. Reflections were integrated and corrected for Lorentz, polarization, and background effects using the Bruker program SAINT. A multi-scan semi-empirical absorption correction was applied using equivalent reflections in SADABS-2012. An initial structure model was obtained by the intrinsic phasing method using SHELXT (Sheldrick 2015) in space group *Pbca* with most atoms located, except some O atoms of water molecules. The SHELXL 2013 software package was used to refine the structure of leesite on the basis of  $F^2$  for unique reflections, and the remaining O atoms of water were located in difference Fourier maps. Hydrogen atom positions were not determined, due to the weak X-ray scattering factor of hydrogen, and the dominance of U in the difference Fourier density maps. Furthermore, the diffraction pattern suffered from a split crystal contribution, with the heaviest contribution to low angle data. An attempt to deconvolute this contribution was made but did not improve the results. The split crystal, in combination with weak diffraction led to some difficulties during refinement of anisotropic displacement parameters for several oxygen atoms, and rigid bond restraints (RIGU) were applied to assist in their refinement. Details regarding the data collection and refinement results are given in the supplementary information<sup>1</sup> and can also be found within the CIF, and bond-valence analysis is given in Appendix<sup>1</sup> Table S4. Powder X-ray diffraction data (Appendix<sup>1</sup> Table S1) and the profile fitting details (Appendix<sup>1</sup> Fig. S4) are available as supplementary information.

## CRYSTAL STRUCTURE DESCRIPTION

### Cation coordination

The structure of leesite (Fig. 3) contains four symmetrically distinct U sites. All adopt sevenfold pentagonal bipyramidal coordination, where the apices of each polyhedron are comprised of multiply bonded oxygen, forming the approximately linear uranyl ion— $\text{UO}_2^{2+}$  (Burns et al. 1997a). Equatorially, each uranyl cation is fivefold-coordinated by O or OH, and the polyhedra are

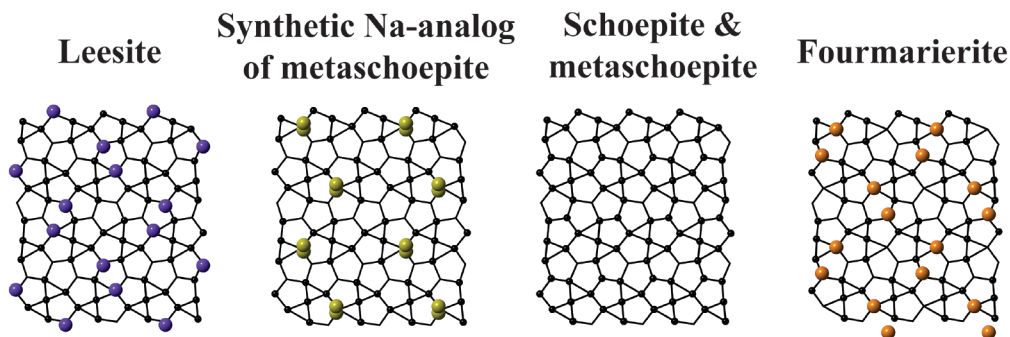


**FIGURE 3.** A comparative view of the anion sheet topologies,  $(\text{OH})^-$  distributions, and cation positions for analogous uranyl-oxide hydroxyhydrates. Black circles highlight vertices containing  $(\text{OH})^-$ , and bare vertices represent  $\text{O}^{2-}$ . The distribution of  $(\text{OH})^-$  in leesite is identical to that of the synthetic Na-analog of metaschoepite. Potassium (blue), lead (orange), and sodium (yellow). (Color online.)

linked by sharing edges arranged into the so-called fourmarierite anion sheet topology (Burns 2005; Li and Burns 2000; Lussier et al. 2016). The sheets in schoepite and metaschoepite also adopt the fourmarierite topology, which consists of sheets built from topological pentagons and triangles (Fig. 3). Pentagons are populated by U atoms, and triangles, arranged in alternating bow-tie arrangements, are vacant.

The interlayer of leesite is populated with  $\text{K}^+$  cations and water molecules. Dimeric clusters of  $\text{K}^+$  and  $\text{H}_2\text{O}$  serve to connect sheets of U polyhedra stacked along  $a$  by coordinating to their outstretched  $\text{O}_{y1}$  atoms (Fig. 4). Coordination about  $\text{K}^+$  is [9]-fold and each  $\text{K}^+$  binds six  $\text{O}_{y1}$  atoms and three water ( $\text{Ow}$ ) molecules, such that the clusters have the composition  $\text{K}_2\text{O}_{10}(\text{H}_2\text{O})_4$ . There is one symmetrically unique K site, and site-scattering refinement reveals it is partially occupied (0.71), in agreement with the average empirical chemistry (0.67 apfu). This is not unexpected, considering the analogous mineral fourmarierite also displays variable  $\text{Pb}^{2+}$  content (0.86–1.02 apfu) in natural and synthetic samples (Li and Burns 2000). Atoms of  $\text{Pb}^{2+}$  in fourmarierite adopt a similar dimeric arrangement in the interlayer—with composition  $\text{Pb}_2\text{O}_{10}(\text{H}_2\text{O})_4$  (Fig. 3).

### Relationship to other UOH minerals

The sheets of uranyl polyhedra in schoepite and metaschoepite are electroneutral, but can accommodate substitution of  $\text{OH}^-$  for  $\text{O}^{2-}$  within the sheet (Finch et al. 1996b). This allows for variably charged sheets and the presence of interlayer cations. A synthetic Na-analog of metaschoepite is known, with an interlayer containing partially occupied  $\text{Na}^+$  sites (Klingensmith et al. 2007). The arrangement of  $\text{OH}^-$  in leesite is identical to that found in the synthetic Na-analog of metaschoepite, and similar to metaschoepite in most regards except that a single  $\text{OH}^-$  group in metaschoepite is deprotonated in leesite (atom O9). Naturally occurring Na-rich metaschoepite is described by Sejkora et al. (2013) from the Jan Evangelista vein, Svornost mine in Jáchymov, and was shown to contain appreciable amounts of other elements (Na, 0.3 apfu; Cu, 0.13 apfu; Al, 0.13 apfu; Pb, 0.08 apfu). The Na-rich material is poorly crystalline and powdery, preventing its formal description as a mineral. Sejkora et al. (2013) also describe K-rich fourmarierite (0.2–0.45 K apfu) from the Evangelista vein, and recently, the schoepite family

mineral kroupaite,  $\text{KPb}_{0.5}[(\text{UO}_2)_8\text{O}_4(\text{OH})_{10}] \cdot 10\text{H}_2\text{O}$ , has been described (Plášil et al. 2017). Structurally, kroupaite is similar to leesite, except  $\text{K}^+$  cations adopt slightly different positions. Presumably, as  $\text{Pb}^{2+}$  content reaches ~50% in these phases, structural transformation to the fourmarierite cell is prompted by interlayer rearrangement and increased  $\text{O}^{2-}$  content within the sheets, however more work is required to understand the relationship between leesite, kroupaite, K-rich fourmarierite, and fourmarierite.

Foord et al. (1997) provide data for an unknown and incompletely characterized phase designated “mineral A” by Frondel (1956) that forms within “gummite” alteration rinds on uraninite from the Ruggles and Palermo granitic pegmatites in New Hampshire, U.S.A. Powder diffraction analyses by Foord et al. (1997) indicate it is a mixture of schoepite-family minerals and other UOH phases. Composite chemical analyses by Foord et al. (1997) indicate the material contains appreciable K, Pb, and Ca; avg. (in wt%)  $\text{UO}_3$  83.5,  $\text{PbO}$  4.85,  $\text{BaO}$  0.68,  $\text{CaO}$  0.167,  $\text{K}_2\text{O}$  2.46,  $\text{SrO}$  0.21,  $\text{ThO}_2$  0.85,  $\text{H}_2\text{O}$  6.9,  $\Sigma 99.62$ . Given the similarity in chemical analyses to leesite, it appears that the mixture of schoepite-family minerals found in some “gummite” could contain leesite.

### BOND VALENCE ANALYSIS AND ROLE OF INTERLAYER $\text{H}_2\text{O}$

The symmetry of minerals in the schoepite family is sensitive to the water content, and presence of cations. Some relations between the cation content and arrangement of interlayer water are revealed by a bond-valence based approach, which examines interactions between the structural unit and the role of interstitial species (Hawthorne 1992; Hawthorne and Schindler 2008; Schindler and Hawthorne 2004, 2008). The approach developed by these authors is a measure termed the charge-deficiency per anion (CDA), and is defined as the average bond-valence per O atom contributed by the interstitial species and adjacent structural units. Stable structures are formed when the bonding availability of the structural unit matches that of the interstitial complex (Hawthorne 2012, 2015). The quantity is useful for crystal-chemical predictions, enabling comparison between minerals with related topologies but differing interlayer constituents.

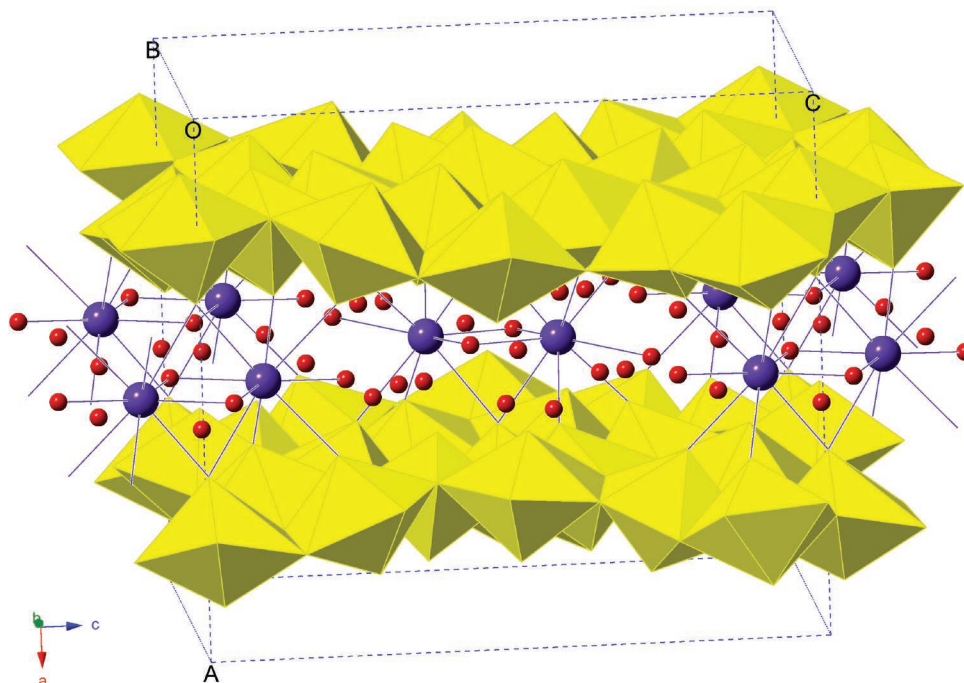


**FIGURE 4.** A polyhedral representation of the uranyl oxide hydroxide sheet (yellow) in leesite, with ball-and-stick interlayer containing water oxygen (red) and potassium (blue). (Color online.)

Bond valence analysis of the X-ray structure permits distinction of O atom types within the structure of leesite, and the ideal structural formula assuming full  $K^+$  occupancy is  $K(H_2O)_2[(UO_2)_4O_2(OH)_5] \cdot 3H_2O$ . The CDA of the sheet in leesite is 0.133, identical to the value for Na-metaschoepite. The value is intermediate to those of schoepite and metaschoepite (0.08) and fourmarierite (0.19). The range in Lewis basicity of the structural unit in leesite is 0.13–0.24 using the method of Schindler and Hawthorne (2008), and is comparable to ranges calculated for other uranyl-oxide hydroxyl-hydrate minerals (e.g., schoepite: 0.11–0.20).

When present in the interstitial complex ( $H_2O$ ) molecules act as transformers of bond-valence from cations within the interlayer to atoms in the structural unit (Schindler and Hawthorne 2008). The interlayer of leesite contains 5 unique ( $H_2O$ ) molecules. The atoms Ow1, Ow2, Ow3, and Ow4 are [5]-coordinated and transfer weak bond valence from  $K^+$  to uranyl ion oxygen atoms within the sheet through various interactions, and according to the designation given by Schindler and Hawthorne (2008), are considered inverse-transformer ( $H_2O$ ) groups. Atom Ow1 forms two bonds to  $K^+$ , two weak H-bonds with uranyl ions of the sheet ( $\sim 0.2$  v.u.), and one H-bond with Ow2. Atoms Ow2, Ow3, and Ow4 each link to two H atoms ( $2 \times 0.8$  v.u.) of other ( $H_2O$ ) molecules, and all form at least one H-bond to uranyl ions of the sheet. They also each accept one H-bond (0.2 v.u.) from (OH) groups of the sheet. The remaining ( $H_2O$ ) group, Ow5, does not bond to a cation and has coordination number [4]. Thus, Ow5 acts as a non-transformer group by propagating weak bond valence from cations to anions that are too distant to bond directly to the cation. Details regarding the number of H-bonds donated and accepted, and their interatomic (O-H $\cdots$ O)

distances are given in Appendix<sup>1</sup> Tables S4 and S5 (Supplementary<sup>1</sup> Information), respectively.

It is difficult to establish if hydronium ( $H_3O^+$ ) is present in schoepite family phases with non-stoichiometric cation contents (Wilkins and Mateen 1974), but this would be in accord with the observation that leesite and other members of the family are formed from acidic solutions. Site-scattering refinement indicates slightly higher  $K^+$  occupancy (0.71) than obtained from LA-ICP-MS analyses (0.67 apfu), which suggests the presence of disordered O ( $H_3O^+$ ) or N ( $NH_4^+$ ) atoms at this site, instead of vacancies. However, the discrepancy in refined occupancy may be related to an inadequate absorption correction. It is currently unclear if partial  $K^+$  occupancy is accounted for by  $OH^- \leftrightarrow O^{2-}$  substitution in the sheet, or through interlayer  $NH_4^+$  or  $H_3O^+$  substitution, but due to their similar sizes,  $H_3O^+$  and  $NH_4^+$  could readily substitute for  $K^+$  in leesite.

#### SPECIATION OF INTERLAYER CATIONS

With details of the range of bonding availability of the structural unit and interlayer ( $H_2O$ ), we now have the necessary information to describe the species of cations that can be expected to occur in the interlayer in schoepite family minerals as demonstrated by Schindler and Hawthorne (2004, 2008). Figure 5 depicts the variation in Lewis acidity for various cation coordination numbers and charges with differing numbers of coordinating transformer ( $H_2O$ ) groups. A stable structure is formed where lines of variable Lewis acidity overlap the Lewis basicity range of the structural unit (shown in blue). As revealed in Figure 5, cations with coordination number  $>[8]$  must bond to at least one inverse-transformer ( $H_2O$ ) group to produce a stable structure (Schindler and Hawthorne 2008). In the structure of leesite,

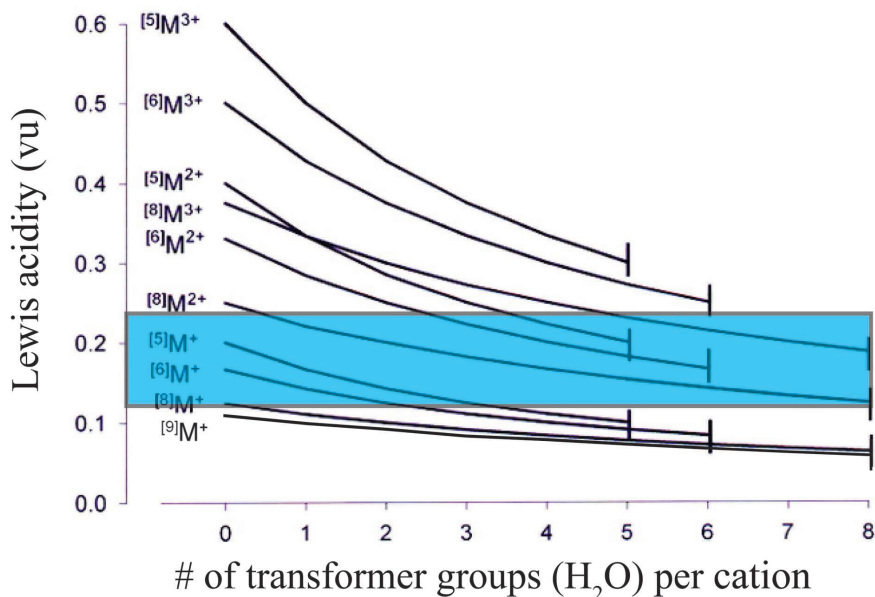


**FIGURE 5.** The variation in Lewis acidity for particular cation coordination numbers and charges of a general interstitial complex with differing numbers of transformer ( $\text{H}_2\text{O}$ ) groups. The range in Lewis basicity of the structural unit of leesite is shown in blue. A stable structure is formed where the lines of variable Lewis acidity overlap the Lewis basicity of the structural unit. Figure adapted in part from Schindler and Hawthorne (2004). (Color online.)

potassium cations are coordinated by three inverse-transformer ( $\text{H}_2\text{O}$ ) groups ( $2 \times \text{Ow}1$ , and  $\text{Ow}3$ ), and this agrees with the predicted coordination number of 0 transformer ( $\text{H}_2\text{O}$ ) groups.

Monovalent cations with a wide range of coordination numbers can be incorporated into the interlayer of leesite, and may include  $\text{H}_3\text{O}^+$ ,  $\text{NH}_4^+$ ,  $\text{Na}^+$ , or  $\text{Cs}^+$ . Incorporation of [8]-coordinated  $\text{Ca}^{2+}$  is possible; however, others have documented conversion of metaschoepite to becquerelite in the presence of  $\text{Ca}^{2+}$  at elevated temperatures (Sandino and Grambow 1994; Sowder et al. 1996, 1999). Although leesite occurs intimately with gypsum, it contains relatively little  $\text{Ca}^{2+}$  (Table 1).  $\text{Ca}$ -rich metaschoepite may be more likely to occur in carbonate-rich assemblages, such as those at the Markey mine to the nearby southwest. Hydrolysis reactions with abundant uranyl carbonates found there may lead to the formation of  $\text{Na}$  or  $\text{Ca}$ -metaschoepite. Samples of  $\text{Na}$ -rich metaschoepite from Jáchymov were shown to contain small amounts of  $\text{Cu}^{2+}$  and  $\text{Al}^{3+}$ , and we can expect these cations will occupy sites that maximize coordination by transformer ( $\text{H}_2\text{O}$ ) groups (Sejkora et al. 2013).

#### RENEWED INTEREST IN PARASCHOEPITE?

In a dry environment, schoepite slowly loses interlayer water (Kubatko et al. 2006; O'Hare et al. 1988), leading to a decrease in the interplanar spacing between sheets as water molecules rearrange and relocate, forming a new H-bonded array in metaschoepite (Weller et al. 2000). Schoep and Stradiot (1947) noted an opaque lemon yellow orthorhombic phase within altered crystals of schoepite, which was indistinguishable from crystals of schoepite except upon determination of its optical properties. A combination of optical and chemical analyses indicated the material is unique from other schoepite family members, with

the formula  $\text{UO}_3 \cdot 1.9\text{H}_2\text{O}$ , and was thus designated paraschoepite. Christ and Clark (1960) report a large interplanar distance ( $c = 15.22 \text{ \AA}$ ) for single crystals of paraschoepite, and state "Because of the distinctive X-ray pattern given by the yellow crystals and the excellent agreement of the optical measurements obtained in the present study with those originally given by Schoep and Stradiot in 1947, there can be little doubt as to the validity of paraschoepite." Subsequent descriptions have attributed paraschoepite to a mixture of metaschoepite, dehydrated schoepite, and ianthinite (Brugger et al. 2011; Finch et al. 1992, 1997); however, the similar large interplanar spacing ( $a = 14.87 \text{ \AA}$ ) and arrangements found in leesite may be in part related to paraschoepite. Leesite contains a predominance of inverse-transformer ( $\text{H}_2\text{O}$ ) groups, which maximize interactions with the sheet in the presence of bulky  $\text{K}^+$  cations. In paraschoepite, interlayer water remaining after partial dehydration would likely rearrange to maximize bonding interactions with the sheet. This is best achieved by the inclusion of more inverse-transformer ( $\text{H}_2\text{O}$ ) group interactions, which are capable of transferring bond strength at longer distances. Finch et al. (1992) argue that paraschoepite represents a metastable structure where localized expansion is associated with the collapse of layers as "dehydrated schoepite" forms. Local expansion of layers may be related to reorganization of interlayer ( $\text{H}_2\text{O}$ ) groups from transformer to inverse-transformer roles, and future X-ray or neutron studies exploring this metastable state may be supplemented by our observations of the structure of leesite.

#### IMPLICATIONS

With the description of leesite, we are better able to recognize the conditions and crystal-chemical features that drive formation

of specific minerals in the schoepite family. Details of the cation arrangement, water content, and H-bonding array can be compared for this series of minerals, and predictions can be made toward possible compositions not yet observed. Our observations of natural samples from several localities reveal that the fourmarierite sheet anion topology is capable of accommodating an interlayer with a range of heterovalent cations and unique configurations. Recognizing how and where large  $K^+$  cations incorporate into this family reveals how short-lived radionuclides like  $^{137}Cs$  or  $^{90}Sr$  will behave during the initial alteration stages of irradiated nuclear fuel (Giammar and Hering 2004). Long-lived radionuclides, such as  $^{135}Cs$  or  $^{237}Np$ , may also be incorporated, albeit under different circumstances. Low-valence cations ( $Cs^+$  and  $Sr^{2+}$ ) will accumulate within interlayer space during formation, or through cation exchange within the interlayer. The incorporation mechanism for high-valence cations (e.g.,  $Np^{5+,6+}$ ,  $Pu^{5+,6+}$ ) depends heavily on the oxidation state, and whether the structure can support substitution of actinyl ions ( $An^{5+,6+}O_2^{1+,2+}$  for uranyl ions  $(UO_2)^{2+}$  within the sheet of polyhedra (Burns et al. 1997b). Incorporation of  $(Np^{5+}O_2)^+$  must be accompanied by an appropriate charge-balancing mechanism; through protonation of the sheet or inclusion of cations (Burns et al. 2004; Klingensmith et al. 2007). Schoepite family phases formed during the initial alteration stages will readily incorporate the elements listed above through these processes, but may be subsequently altered or undergo structural rearrangement. For example, Sandino and Grambow (1994) observed the complete conversion of metaschoepite into compreignacite in the presence of excess  $K^+$  at room temperature. Leesite from the Jomac mine is intimately associated with compreignacite, and facile conversion to compreignacite may explain the rarity of leesite. In this case, the crystal-chemical predictability afforded by the bond-valence approach is very powerful due to the penchant for UOH minerals to form, rearrange, and redistribute U or cations (Finch et al. 1992).

#### ACKNOWLEDGMENTS

This research is funded by the Office of Basic Energy Sciences of the U.S. Department of Energy as part of the Materials Science of Actinides Energy Frontier Research Center (DE-SC0001089). The Element2 HR-ICP-MS instrument used for chemical analyses is housed within the Midwest Isotope and Trace Element Research Analytical Center (MITERAC) at the University of Notre Dame. Electron microscopy was carried out in the Applied Chemical and Morphological Analysis Laboratory at Michigan Technological University. The John Jago Trelawney Endowment to the Mineral Sciences Department of the Natural History Museum of Los Angeles County funded a portion of this study. Jakub Plášil is thankful for the support from the project GACR 15-12653S.

#### REFERENCES CITED

- Amonette, J.E., Holdren, G.R. Jr., Krupa, K.M., and Lindenmeier, C.W. (1994) Assessing the Environmental Availability of Uranium in Soils and Sediments. NUREG/CR-6232 PNL-9570, Pacific Northwest Laboratory, Richland, Washington, [http://www.iaea.org/inis/collection/NCLCollectionStore/\\_Public/25/069/25069667.pdf?r=1](http://www.iaea.org/inis/collection/NCLCollectionStore/_Public/25/069/25069667.pdf?r=1). Accessed: August 13, 2017. (Archived by WebCite at <http://www.webcitation.org/6shXVIKZO>).
- Bartlett, J.R., and Cooney, R.P. (1989) On the determination of uranium-oxygen bond lengths in dioxouranium(VI) compounds by Raman spectroscopy. *Journal of Molecular Structure*, 193, 295–300.
- Brugger, J., Meisser, N., Etschmann, B., Ansermet, S., and Pring, A. (2011) Paulscherrite from the Number 2 Workings, Mount Painter Inlier, Northern Flinders Ranges, South Australia: “Dehydrated schoepite” is a mineral after all. *American Mineralogist*, 96, 229–240.
- Burns, P.C. (2005)  $U^{6+}$  minerals and inorganic compounds: Insights into an expanded structural hierarchy of crystal structures. *Canadian Mineralogist*, 43(6), 1839–1894.
- Burns, P.C., Ewing, R.C., and Hawthorne, F.C. (1997a) The crystal chemistry of hexavalent uranium; polyhedron geometries, bond-valence parameters, and polymerization of polyhedra. *Canadian Mineralogist*, 35(6), 1551–1570.
- Burns, P.C., Ewing, R.C., and Miller, M.L. (1997b) Incorporation mechanisms of actinide elements into the structures of  $U^{6+}$  phases formed during the oxidation of spent nuclear fuel. *Journal of Nuclear Materials*, 245(1), 1–9.
- Burns, P.C., Deely, K.M., and Skanthakumar, S. (2004) Neptunium incorporation into uranyl compounds that form as alteration products of spent nuclear fuel: Implications for geologic repository performance. *Radiochimica Acta*, 92(3), 151–159.
- Čejka, J. (1999) Infrared spectroscopy and thermal analysis of the uranyl minerals. In P.C. Burns and R.C. Ewing, Eds., *Uranium: Mineralogy, Geochemistry and the Environment*, 38, p. 521–622. Mineralogical Society of America.
- Christ, C.L., and Clark, J.R. (1960) Crystal chemical studies of some uranyl oxide hydrates. *American Mineralogist*, 45, 1026–1061.
- Dothée, D.G., and Camelot, M.M. (1982) Vibrational spectroscopy of potassium hexauranate hydrate. I. Frequencies assignable to oxygen-atoms motions—hypothesis on the structure of the anionic layer. *Bulletin de la Société chimique de France* (3-4), 97–102.
- Dothée, D.G., Fahys, B.R., and Camelot, M.M. (1982) Vibrational spectroscopy of potassium hexauranate hydrate. II. Motions of hydrogen atoms—hypothesis on the water-structure in the uranate. *Bulletin de la Société chimique de France* (3-4), 103–108.
- Finch, R.J., and Ewing, R.C. (1992) The corrosion of uraninite under oxidizing conditions. *Journal of Nuclear Materials*, 190, 133–156.
- Finch, R.J., and Murakami, T. (1999) Systematics and paragenesis of uranium minerals. In P.C. Burns and R.C. Ewing, Eds., *Uranium: Mineralogy, Geochemistry and the Environment*, 38, 91–179. Reviews in Mineralogy, Mineralogical Society of America, Chantilly, Virginia.
- Finch, R.J., Miller, M.L., and Ewing, R.C. (1992) Weathering of natural uranyl oxide hydrates—schoepite polytypes and dehydration effects. *Radiochimica Acta*, 58-9, 433–443.
- Finch, K.J., Suksi, J., Rasilainen, K., and Ewing, R.C. (1996a) Uranium-series ages of secondary uranium minerals with applications to the long-term evolution of spent nuclear fuel. In W.M. Murphy and D.A. Knecht, Eds. *Scientific Basis for Nuclear Waste Management XIX*, 412, 823–830. Materials Research Society, Pittsburgh.
- Finch, R.J., Cooper, M.A., Hawthorne, F.C., and Ewing, R.C. (1996b) The crystal structure of schoepite,  $[(UO_2)_8O_2(OH)_{12}](H_2O)_{12}$ . *Canadian Mineralogist*, 34, 1071–1088.
- Finch, R.J., Hawthorne, F.C., Miller, M.L., and Ewing, R.C. (1997) Distinguishing among schoepite,  $[(UO_2)_8O_2(OH)_{12}](H_2O)_{12}$ , and related minerals by X-ray powder diffraction. *Powder Diffraction*, 12(4), 230–238.
- Foord, E.E., Korzeb, S.L., Lichte, F.E., and Fitzpatrick, J.J. (1997) Additional studies on mixed uranyl oxide-hydroxide hydrate alteration products of uraninite from the Palermo and Ruggles granitic pegmatites, Grafton County, New Hampshire. *Canadian Mineralogist*, 35, 145–151.
- Fronzel, C. (1956) Mineral composition of gummite. *American Mineralogist*, 41, 539–568.
- Frost, R.L., Čejka, J., and Weier, M.L. (2007) Raman spectroscopic study of the uranyl oxyhydroxide hydrates: becquerelite, billietite, curite, schoepite and vandriesscheite. *Journal of Raman Spectroscopy*, 38, 460–466.
- Giammar, D.E., and Hering, J.G. (2004) Influence of dissolved sodium and cesium on uranyl oxide hydrate solubility. *Environmental Science & Technology*, 38(1), 171–179.
- Hawthorne, F.C. (1992) The role of OH and  $H_2O$  in oxide and oxysalt minerals. *Zeitschrift für Kristallographie*, 201(3-4), 183–206.
- (2012) A bond-topological approach to theoretical mineralogy: crystal structure, chemical composition and chemical reactions. *Physics and Chemistry of Minerals*, 39(10), 841–874.
- (2015) Toward theoretical mineralogy: A bond-topological approach. *American Mineralogist*, 100, 696–713.
- Hawthorne, F.C., and Schindler, M. (2008) Understanding the weakly bonded constituents in oxysalt minerals. *Zeitschrift für Kristallographie-Crystalline Materials*, 223, 41.
- Haynes, P.E. (2000) Mineralogy of the Jomac Mine, San Juan county, Utah. *Rocks and Minerals*, 75(4), 240–248.
- Klingensmith, A.L., Deely, K.M., Kinman, W.S., Kelly, V., and Burns, P.C. (2007) Neptunium incorporation in sodium-substituted metaschoepite. *American Mineralogist*, 92, 662–669.
- Kubatko, K.A., Helean, K., Navrotsky, A., and Burns, P.C. (2006) Thermodynamics of uranyl minerals: Enthalpies of formation of uranyl oxide hydrates. *American Mineralogist*, 91, 658–666.
- Li, Y., and Burns, P.C. (2000) Investigations of crystal-chemical variability in lead uranyl oxide hydrates. II. Fourmarierite. *Canadian Mineralogist*, 38(3), 737–749.
- Libowitzky, E. (1999) Correlation of O-H stretching frequencies and O-H...O hydrogen bond lengths in minerals. *Monatshefte Für Chemie*, 130(8), 1047–1059.
- Lussier, A.J., Burns, P.C., and King-Lopez, R. (2016) A revised and expanded structure hierarchy of natural and synthetic hexavalent uranium compounds. *Canadian Mineralogist*, 54(1), 177–283.

- Mandarino, J.A. (2007) The Gladstone-Dale compatibility of minerals and its use in selecting mineral species for further study. *Canadian Mineralogist*, 45, 1307–1324.
- O'Hare, P.A.G., Lewis, B.M., and Nguyen, S.N. (1988) Thermochemistry of uranium compounds XVII. Standard molar enthalpy of formation at 198.15 K of dehydrated schoepite  $UO_3 \cdot 0.9 H_2O$ . Thermodynamics of (schoepite + dehydrated schoepite + water). *Journal of Chemical Thermodynamics*, 20(11), 1287–1296.
- Plášil, J. (2014) Oxidation-hydration weathering of uraninite: the current state-of-knowledge. *Journal of Geosciences*, 59(2), 99–114.
- Plášil, J., Škoda, R., Čejka, J., Bourgoin, V., and Boulliard, J.-C. (2016) Crystal structure of the uranyl-oxide mineral rameauite. *European Journal of Mineralogy*, 28, 959–967.
- Plášil, J., Kampf, A.R., Olds, T.A., Sejkora, J., Škoda, R., Burns, P.C., and Čejka, J. (2017) Kroupaite, IMA 2017-031. *CNMNC Newsletter No. 38*, Aug 2016; *Mineralogical Magazine*, 81(4), 1033–1038.
- Sandino, M.C.A., and Grambow, B. (1994) Solubility equilibria in the U(VI)-Ca-K-Cl-H<sub>2</sub>O system: transformation of schoepite into becquerelite and compreignacite. *Radiochimica Acta*, 66-7, 37–43.
- Schindler, M., and Hawthorne, F.C. (2004) A bond-valence approach to the uranyl-oxide hydroxy-hydrate minerals: Chemical composition and occurrence. *Canadian Mineralogist*, 42(6), 1601–1627.
- (2008) The stereochemistry and chemical composition of interstitial complexes in uranyl-oxysalt minerals. *Canadian Mineralogist*, 46(2), 467–501.
- Schoep, A., and Stradiot, S. (1947) Paraschoepite and epianthinite, two new uranium minerals from Shinkolobwe (Belgian Congo). *American Mineralogist*, 32, 344–350.
- Sejkora, J., Plášil, J., and Bureš, B. (2013) Unusual association of supergene uranium minerals from the Jan Evangelista vein, Jáchymov (Czech Republic). *Bulletin mineralogicko-petrologického oddělení Národního Muzea (Praha)*, 21, 143–156.
- Sheldrick, G.M. (2015) SHELXT—Integrated space-group and crystal-structure determination. *Acta Crystallographica*, A71, 3–8.
- Sowder, A.G., Clark, S.B., and Fjeld, R.A. (1996) The effect of silica and phosphate on the transformation of schoepite to becquerelite and other uranyl phases. *Radiochimica Acta*, 74, 45–49.
- (1999) The transformation of uranyl oxide hydrates: The effect of dehydration on synthetic metaschoepite and its alteration to becquerelite. *Environmental Science & Technology*, 33(20), 3552–3557.
- Taylor, J.C., and Hurst, H.J. (1971) The hydrogen-atom locations in the  $\alpha$  and  $\beta$  forms of uranyl hydroxide. *Acta Crystallographica*, B27(10), 2018–2022.
- Trites, A.F. Jr., and Hadd, G.A. (1958) Geology of the Jomac Mine, White canyon area, San Juan county, Utah. U.S. Geological Survey Bulletin, 1046-H.
- Vochten, R., and Deliens, M. (1998) Blatonite,  $UO_2CO_3 \cdot H_2O$ , a new uranyl carbonate monohydrate from San Juan County, Utah. *Canadian Mineralogist*, 36, 1077–1081.
- Vochten, R., Deliens, M., and Medenbach, O. (2001) Oswaldpeetersite  $(UO_2)_2CO_3(OH)_2(H_2O)_4$ , a new basic uranyl carbonate mineral from the Jomac uranium mine, San Juan County, Utah, USA. *Canadian Mineralogist*, 39, 1685–1689.
- Walenta, K., and Theye, T. (2012) Heisenbergite, a new uranium mineral from the uranium deposit of Menzenschwand in the Southern Black Forest, Germany. *Neues Jahrbuch für Mineralogie*, 189(2), 117–123.
- Walker, T.L. (1923) Schoepite, a new uranium mineral from Kasolo, Belgian Congo. *American Mineralogist*, 8, 67–69.
- Weller, M.T., Light, M.E., and Gelbrich, T. (2000) Structure of uranium(VI) oxide dihydrate,  $UO_3 \cdot 2H_2O$ ; synthetic meta-schoepite  $(UO_2)_4O(OH)_6 \cdot 5H_2O$ . *Acta Crystallographica*, B56, 577–583.
- Wilkins, R.W.T., and Mateen, A. (1974) The spectroscopic study of oxonium ions in minerals. *American Mineralogist*, 59, 811–819.
- Wood, R.M., and Palenik, G.J. (1999) Bond valence sums in coordination chemistry using new  $R_0$  values. Potassium-oxygen complexes. *Inorganic Chemistry*, 38(5), 1031–1034.
- Wronkiewicz, D.J., Bates, J.K., Gerding, T.J., Veleckis, E., and Tani, B.S. (1992) Uranium release and secondary phase formation during unsaturated testing of  $UO_2$  at 90°C. *Journal of Nuclear Materials*, 190, 107–127.

MANUSCRIPT RECEIVED JANUARY 19, 2017  
 MANUSCRIPT ACCEPTED SEPTEMBER 16, 2017  
 MANUSCRIPT HANDLED BY MARTIN KUNZ

#### Endnote:

<sup>1</sup>Deposit item AM-18-16083, CIF and Supplemental Material. Deposit items are free to all readers and found on the MSA web site, via the specific issue's Table of Contents (go to [http://www.minsocam.org/MSA/AmMin/TOC/2018/Jan2018\\_data/Jan2018\\_data.html](http://www.minsocam.org/MSA/AmMin/TOC/2018/Jan2018_data/Jan2018_data.html)).